Differences in Glycinergic mIPSCs in the Auditory Brain Stem of Normal and Congenitally Deaf Neonatal Mice

Richardson N. Leao, Sharon Oleskevich, Hong Sun, Melissa Bautista, Robert E.W. Fyffe and Bruce Walmsley

J Neurophysiol 91:1006-1012, 2004. First published 15 October 2003; doi:10.1152/jn.00771.2003

Journal of Neurophysiology publishes original articles on the function of the nervous system. It is published 12 times a year (monthly) by the American Physiological Society, 9650 Rockville Pike, Bethesda MD 20814-3991. ISSN: 0022-3077, ESSN: 1522-1598. Visit our website at http://www.the-aps.org/.

J Neurophysiol 91: 1006–1012, 2004;
10.1152/jn.00771.2003.

Differences in Glycinergic mIPSCs in the Auditory Brain Stem of Normal and Congenitally Deaf Neonatal Mice

Richardson N. Leao,[1] Sharon Oleskevich,[1] Hong Sun,[2] Melissa Bautista,[2] Robert E. W. Fyffe,[2] and Bruce Walmsley[1]

[1]*Synaptic Structure and Function Group, Division of Neuroscience, The John Curtin School of Medical Research, The Australian National University, Canberra ACT 0200, Australia; and* [2]*Center for Brain Research, Wright State University, Dayton, Ohio 45435*

Submitted 7 August 2003; accepted in final form 2 October 2003

Leao, Richardson N., Sharon Oleskevich, Hong Sun, Melissa Bautista, Robert E. W. Fyffe, and Bruce Walmsley. Differences in glycinergic mIPSCs in the auditory brain stem of normal and congenitally deaf neonatal mice. *J Neurophysiol* 91: 1006–1012, 2004; 10.1152/jn.00771.2003. We have investigated the fundamental properties of central auditory glycinergic synapses in early postnatal development in normal and congenitally deaf (*dn/dn*) mice. Glycinergic miniature inhibitory postsynaptic currents (mIPSCs) were recorded using patch-clamp methods in neurons from a brain slice preparation of the medial nucleus of the trapezoid body (MNTB), at 12–14 days postnatal age. Our results show a number of significant differences between normal and deaf mice. The frequency of mIPSCs is greater (50%) in deaf versus normal mice. Mean mIPSC amplitude is smaller in deaf mice than in normal mice (mean mIPSC amplitude: deaf, 64 pA; normal, 106 pA). Peak-scaled fluctuation analysis of mIPSCs showed that mean single channel conductance is greater in the deaf mice (deaf, 64 pS; normal, 45 pS). The mean decay time course of mIPSCs is slower in MNTB neurons from deaf mice (mean half-width: deaf, 2.9 ms; normal, 2.3 ms). Light- and electron-microscopic immunolabeling results showed that MNTB neurons from deaf mice have more (30%) inhibitory synaptic sites (postsynaptic gephyrin clusters) than MNTB neurons in normal mice. Our results demonstrate substantial differences in glycinergic transmission in normal and congenitally deaf mice, supporting a role for activity during development in regulating both synaptic structure (connectivity) and the fundamental (quantal) properties of mIPSCs at central glycinergic synapses.

INTRODUCTION

During development, both activity-dependent and activity-independent processes regulate synaptic connections and neuronal membrane properties (Friauf and Lohmann 1999). An essential first step in understanding these processes is to reveal which particular synaptic and neuronal properties are sensitive to modification by activity during development. The auditory system offers a potentially valuable means of studying the effects of altered activity on synaptic and neuronal properties in central pathways, since auditory nerve input to the brain can be easily and effectively manipulated. Auditory nerve activity can be eliminated either by mechanical or chemical disruption or ablation of the cochlea or by the use of congenitally deaf animals with cochlear dysfunction. A number of previous studies have revealed changes in the morphology and function of central auditory pathways following cochlear disruption (Friauf and Lohmann 1999; Rubel and Fritzsch 2002; Sanes and Friauf 2000). Francis and Manis (2000) have provided one of the few studies on detailed changes in membrane properties following bilateral cochlear ablation, in an investigation of the electrical properties of ventral cochlear nucleus (VCN) cells in rat brain stem slices. However, there is very little information on the effects of cochlear dysfunction on central synaptic transmission, in particular at the detailed quantal level. A knowledge of these differences is potentially important for understanding activity-dependent regulation of synapses and the central processing of signals transmitted via auditory nerve stimulation in hereditary deafness.

The congenitally deaf *dn/dn* mouse has been used as a valuable model of human hereditary deafness and is a naturally occurring mutant strain exhibiting cochlear hair cell dysfunction from birth, with no evidence for spontaneous or acoustically evoked auditory nerve activity (Bock et al. 1982; Durham et al. 1989; Keats and Berlin 1999; Steel and Bock 1980). Our recent results have demonstrated significant differences in the excitatory auditory nerve–bushy cell synapse (the endbulb of Held) in the anteroventral cochlear nucleus (AVCN) of normal and *dn/dn* mice (Oleskevich and Walmsley 2002). The results showed that, despite a lack of auditory nerve activity, synaptic strength was increased at this synapse in the *dn/dn* mouse, primarily due to a greater presynaptic release probability (Oleskevich and Walmsley 2002). However, no difference was observed in the properties of the quantal excitatory synaptic currents generated at this synaptic connection. In the present study, we have extended our investigations to a study of inhibitory glycinergic transmission.

Previous studies have demonstrated the advantages of investigating auditory brain stem neurons, in particular AVCN bushy cells and principal neurons of the medial nucleus of the trapezoid body (MNTB), for the study of both excitatory and inhibitory transmission (Forsythe and Barnes-Davies 1993; Isaacson and Walmsley 1995; Lim et al. 1999, 2000, 2003; Schneggenburger et al. 2002). Both of these cell types exhibit simple morphologies with round or oval cell bodies and one or several small tufted dendrites. The vast majority of synaptic contacts, both excitatory (the glutamatergic endbulbs and calyces of Held) and inhibitory (both glycinergic and GABAergic), are made with the cell soma, thus avoiding electrotonic complications in the interpretation of synaptic current recordings. In AVCN bushy cells, a correlation has been shown

Address for reprint requests and other correspondence: B. Walmsley, The Synaptic Structure and Function Group, Division of Neuroscience, The John Curtin School of Medical Research, The Australian National University, PO Box 334, Canberra ACT 2601, Australia (E-mail: Bruce.Walmsley@anu.edu.au).

The costs of publication of this article were defrayed in part by the payment of page charges. The article must therefore be hereby marked "*advertisement*" in accordance with 18 U.S.C. Section 1734 solely to indicate this fact.

between miniature inhibitory postsynaptic current (mIPSC) amplitude and mean glycine receptor cluster size, thus establishing a direct link between structure and function at these synapses (Lim et al. 1999). Studies in tissue culture have demonstrated that the clustering of glycine receptors can be modified by presynaptic nerve activity, in a process involving the entry of calcium into the postsynaptic neuron (Craig 1998; Kirsch and Betz 1998). Thus nerve activity during development is likely to be very important in regulating glycinergic synaptic transmission (Sanes and Friauf 2000). In this study, we have investigated glycinergic transmission in MNTB principal cells in congenitally deaf mice. Our results reveal significant differences in both the physiological and morphological properties of glycinergic synaptic connections between normal and congenitally deaf mice and provide insight into the role of neural activity during development in regulating inhibitory synaptic properties at the quantal level.

METHODS

Electrophysiology

Normal (CBA strain, 12–14 days postnatal) and congenitally deaf (*dn/dn* with CBA background, 12–14 days postnatal) mice were decapitated without anesthetic in accordance with the Australian National University Animal Ethics Committee protocol. The brain was removed and placed in ice-cold low-calcium artificial cerebrospinal fluid (ACSF in mM: 130 NaCl, 3.0 KCl, 5.0 $MgCl_2$, 1.0 $CaCl_2$, 1.25 NaH_2PO, 26.2 $NaHCO_3$, 10 glucose, equilibrated with 95% O_2, 5% CO_2). Transverse slices (150 μm) were made of the medial nucleus of the trapezoid body (MNTB) using an EMS (USA) oscillating tissue slicer, as previously described (Lim et al. 2003). Slices were incubated for 1 h in normal ACSF (in mM: 130 NaCl, 3.0 KCl, 1.3 Mg_2SO_4, 2.0 $CaCl_2$, 1.25 NaH_2PO_4, 26.2 $NaHCO_3$, 10 glucose, equilibrated with 95% O_2–5% CO_2) at 35°C and subsequently held at room temperature (22–25°C) for electrophysiological recording. Whole cell patch electrode recordings (at a membrane potential of −60 mV) were made from MNTB neurons visualized in the slices using infrared differential interference contrast optics. Patch electrodes (3–5 MΩ resistance) were pulled from borosilicate hematocrit glass tubing using a two-stage Narashige puller (Japan). Patch-pipettes contained (in mM) 120 CsCl, 4 NaCl, 4 $MgCl_2$, 0.001 $CaCl_2$, 10 HEPES, 3 Mg–ATP, 0.1 GTP–Tris, and 0.2–10 EGTA (pH adjusted to 7.2 using CsOh). Osmolarity, when necessary, was adjusted to 290–300 mOsm with sorbitol. Series resistance, which was <10 MΩ, was routinely compensated by >80%. Synaptic currents were recorded and filtered at 10 kHz with an Axopatch 1-D amplifier (Axon Inst.) before being digitized at 20 kHz. Data were also recorded on video tape with a VCR (Vetter) and digitized off-line. Data acquisition and analysis was performed using Axograph (Axon Inst.). The amplitudes of spontaneous IPSCs were measured using semiautomated detection procedures (Axograph 4.0), as previously described (Clements and Bekkers 1997; Lim et al. 2003). Results are expressed as mean ± SE. Unless otherwise indicated, significance of results was assessed using a paired *t*-test, with significance indicated by $P < 0.05$. (Other tests used were Spearman or Kendall nonparametric correlation tests, and the Kolmogorov–Smirnov test.)

Single channel conductance was estimated using peak-scaled fluctuation analysis of mIPSCs, according to the method of Traynelis et al. (1993) (see also Singer and Berger 1999 for glycinergic mIPSCs). For each cell, the mean time course of mIPSCs was determined by averaging individual mIPSCs aligned on their rising phase. For each individual mIPSC, the mean mIPSC was scaled to the peak and subtracted. This operation was performed for all of the mIPSCs recorded in the cell, and a plot of variance versus mean current was constructed. A linear regression line through the origin was fitted to the initial phase (25%) of the variance–mean plot, the slope of which represents a measure of the mean single channel current (weighted by the subconductance states) (Traynelis et al. 1993).

Drugs were added to the perfusate, as indicated: 6-cyano-7-nitroquinoxaline-2,3-dione (CNQX; Tocris), (±)-2-amino-5-phosphonopentanoic acid (D-AP5; RBI), bicuculline methochloride (Tocris), strychnine hydrochloride (Sigma), TTX (Alamone). Spontaneous glycinergic mIPSCs were isolated by the use of TTX (1 μM), CNQX (10 μM), D-AP5 (30 μM), and bicuculline methochloride (10 μM). Where indicated, ruthenium red (100 μM) was added to the extracellular solution to increase the frequency of spontaneous mIPSCs (Lim et al. 2003). Initial experiments were also carried out to assess the contribution of GABA versus glycine receptor-mediated components of postsynaptic currents in MNTB neurons. Evoked IPSCs were elicited using a bipolar extracellular electrode placed close to the midline. Stimulus strength was adjusted between 10 and 20 V to give a stable response for both normal and deaf mice. Bicuculline (10 μM) and strychnine (0.5 μM) were then added sequentially (and, in several experiments, in reverse order) to assess the contributions of GABAergic and glycinergic currents, respectively.

Light and electron microscopic immunohistochemistry

Normal CBA and deaf *dn/dn* mice (13 days postnatal age) were killed with an overdose of pentobarbital sodium (>80 mg/kg) and perfused via the left ventricle with cold vascular rinse (0.01 M phosphate buffer with 137 mM NaCl, 3.4 mM KCl, and 6 mM $NaHCO_3$) followed by fixative (4% paraformaldehyde for confocal microscopy, 4% paraformaldehyde/0.5% glutaraldehyde for preembedding immunoelectron microscopy, in 0.1 M phosphate buffer; pH 7.4) for 10–15 min. For immunofluorescence, transverse sections (30 μm thick) of the brain stem were obtained at the level of MNTB on a freezing sliding microtome and mounted on gelatin-coated slides. After washing, the sections were incubated in mouse mAb 7a (anti-gephyrin; 1:100 dilution; Boehringer Mannheim, Indianapolis, IN) overnight, and then for 2 h in FITC- or Cy3-conjugated goat anti-mouse IgG (1:50; Jackson, West Grove, PA), and coverslipped with fluorescence mounting medium (Vectashield, Vector, Burlingame, CA).

In experiments to visualize and count gephyrin clusters, MNTB neurons were visualized with fluorescent Nissl staining. To determine the relationship of gephyrin clusters to inhibitory synaptic terminals, a series of dual immunostaining experiments were performed using tissue from older (7 wk) animals, in which gephyrin immunolabeling was combined with labeling against a marker of glycinergic (guinea pig anti-GlyT2, Chemicon, 1:1000 dilution) or GABAergic (mouse anti-GAD65, BD Pharmingen, 1:200 or rabbit anti-GAD67, Chemicon, 1:200) presynaptic terminals, using appropriate combinations of secondary antibodies. Preparations were imaged using a laser scanning confocal microscope (Olympus Fluoview) equipped with a ×60 oil immersion objective (N.A. 1.4). Series of optical section separated by 0.5–1.0 μm in the *z*-axis were acquired throughout whole cells to permit counting of punctate surface immunolabeling. Counting of discrete clusters was performed using ImagePro version 4.1. For preembedding immunohistochemistry and ultrastructural analysis, gephyrin immunostaining was revealed as previously described (Alvarez et al. 1997), and ultrathin sections were viewed on a Phillips EM 208S. Low-power electron micrographs of MNTB neurons and high-power images of gephyrin-labeled synaptic sites were produced using ImagePro version 4.1.

RESULTS

Results were obtained using whole cell recordings from MNTB neurons in slices from age-matched (12–14 days postnatal) normal and congenitally deaf mice.

Inhibitory transmission is predominantly glycinergic in MNTB neurons of both normal and deaf mice

Nerve terminals containing glycine and GABA have been demonstrated on brain stem auditory neurons, including MNTB principal neurons and AVCN bushy cells (Helfert et al. 1989). Other studies have reported a developmental increase in the proportion of glycinergic to GABAergic transmission in auditory brain stem nuclei (Kotak et al. 1998). In AVCN bushy cells, postsynaptic inhibition is predominantly glycinergic at about 2 wk postnatal (Lim et al. 2000). In the present study, the relative contributions of glycine and GABA currents to postsynaptic inhibition have been measured in MNTB neurons of normal and deaf mice (Fig. 1).

The proportion of glycinergic versus GABAergic synaptic current in mouse MNTB neurons was examined by using extracellular (multifiber) stimulation to evoke IPSCs (see also Lim et al. 2000). Addition of 10 μM bicuculline to block $GABA_A$ receptors produced a small decrease in the amplitude of evoked IPSCs in MNTB neurons of normal (to 80% of control, $n = 8$ cells) and deaf mice (to 95% of control, $n = 8$ cells). Subsequent addition of 0.5 μM strychnine completely blocked the remaining IPSC in both normal and deaf mice (Fig. 1, *A* and *B*). (The predominance of glycinergic current compared with GABAergic current was confirmed by applying strychnine first, followed by bicuculline. Application of strychnine resulted in a block to 12% of control evoked IPSC for normal mice ($n = 2$) and 5% of control evoked IPSC for deaf mice ($n = 2$).) Because of potential time course differences between glycinergic and GABAergic currents, the area (charge) of the evoked excitatory postsynaptic currents (EPSCs) before and after bicuculline was also measured. GABAergic current contributed 18.5% ($n = 8$) to the evoked EPSC area in control mice and 25.8% ($n = 8$) to the evoked EPSC area in deaf mice. The time constant of the decay phase of evoked IPSCs was longer in deaf mice, although this difference was not significant (time constant; normal, 5.42 $\pm$ 0.19 ms, $n = 8$; deaf, 8.01 $\pm$ 0.14 ms, $n = 8$; $P = 0.07$). These results indicate that inhibitory transmission in MNTB neurons is predominantly glycinergic in both normal (CBA) and deaf (*dn/dn*) mice. The remainder of the results are concerned exclusively with aspects of glycinergic transmission in MNTB neurons and, unless stated otherwise, reference to IPSCs or mIPSCs will imply glycinergic IPSCs or glycinergic mIPSCs.

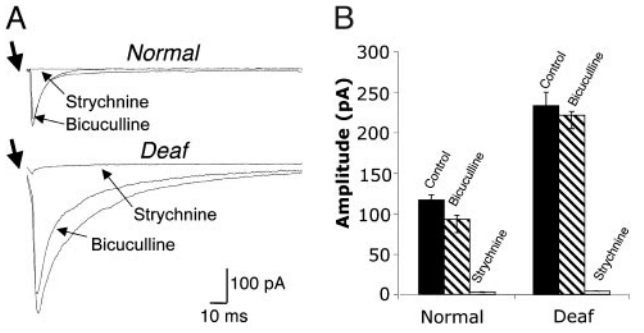

FIG. 1. Inhibitory transmission in both normal and congenitally deaf (*dn/dn*) mice is predominantly mediated by glycine receptors. *A*: whole cell recordings in medial nucleus of the trapezoid body (MNTB) neurons of inhibitory postsynaptic currents (IPSCs) evoked by extracellular stimulation in slices from normal mice (*top*) and deaf (*dn/dn*) mice (*bottom*), at 12–14 days postnatal age. Addition of bicuculline (10 μM) caused a small decrease in IPSC amplitude. Subsequent addition of strychnine (0.5 μM) resulted in a complete block of the IPSCs. Stimulus artifacts have been blanked at arrows. *B*: mean effects of bicuculline (10 μM) and strychnine (0.5 μM) on the peak amplitude of evoked IPSCs in MNTB neurons from normal mice ($n = 8$ cells) and deaf mice ($n = 8$ cells).

MNTB neurons in deaf mice exhibit more postsynaptic inhibitory synaptic sites

To examine possible structural differences in the inhibitory synaptic connections with MNTB neurons in deaf mice, immunolabeling of the inhibitory receptor clustering protein gephyrin was carried out. Normal mice (CBA, 13 days postnatal, $n = 20$ cells, 2 mice) and deaf mice (*dn/dn*, 13 days postnatal, $n = 20$ cells, 2 mice) were fixed and processed for immunohistochemistry (see METHODS). As shown in Fig. 2*A* and *B*, gephyrin-immunoreactive clusters were located over the surface of MNTB cell bodies and were of variable size, shape, and complexity, ranging from small spots to large structures that have complex shape with and without perforations. In both normal and deaf mice, the majority of surface membrane clusters were apposed by presynaptic terminals positively labeled by an antibody against the glycine transporter (GlyT2, Fig. 2, *C* and *D*). A smaller proportion of clusters are apposed by GABAergic terminals (not shown) and taken together these results suggest that essentially all gephyrin clusters are apposed by glycinergic or GABAergic terminals, and thus that they represent discrete inhibitory synapses. There is relatively little overlap in the MNTB between GlyT2- and GAD-labeled axons and terminals (not shown). Ultrastructural analysis in deaf mice (Fig. 2, *E* and *F*) confirmed that all of the gephyrin immunolabeling is present in the MNTB neuron somatic surface membrane. Moreover, the gephyrin immunoreactivity is exclusively localized at synaptic sites, confirming the close correspondence between discrete surface membrane gephyrin clusters and glycinergic/GABAergic synaptic sites observed in other studies (Alvarez et al. 1997; Lim et al. 1999, 2000). The apposed presynaptic terminals (Fig. 2, *E* and *F*) are noncalyceal, and likely represent inhibitory synapses. There is no labeling of extrasynaptic membrane or of presynaptic structures. Similar results were observed in ultrastructural analysis of gephyrin-labeled MNTB neurons in normal mice (not shown). Using confocal microscopy, immunofluorescent clusters ($n = 2295$) were counted on 20 MNTB neurons from normal mice and 20 MNTB neurons from deaf mice. MNTB neurons in deaf mice displayed a significantly larger (30%) number of discrete gephyrin clusters than neurons in normal mice (means, 61.9 $\pm$ 10.5 vs. 47.9 $\pm$ 7.1; $P < 0.01$). Thus the immunolabeling data indicate that there are significantly more inhibitory synaptic sites on MNTB neurons in deaf mice than in age-matched normal mice.

Glycinergic mIPSC frequency and amplitude are greater in deaf mice

Figure 3 shows results of glycinergic mIPSCs recorded in MNTB neurons in the presence of TTX (1 μM), CNQX (10 μM), D-AP5 (30 μM), bicuculline (10 μM), and ruthenium red (100 μM) (Lim et al. 2003). Mean mIPSC frequency was significantly greater (53%) in deaf versus normal mice (deaf, 1.38 $\pm$ 0.03 Hz, $n = 18$ cells; normal, 0.9 $\pm$ 0.05, $n = 18$ cells; $P < 0.03$). A higher mIPSC frequency is consistent with the

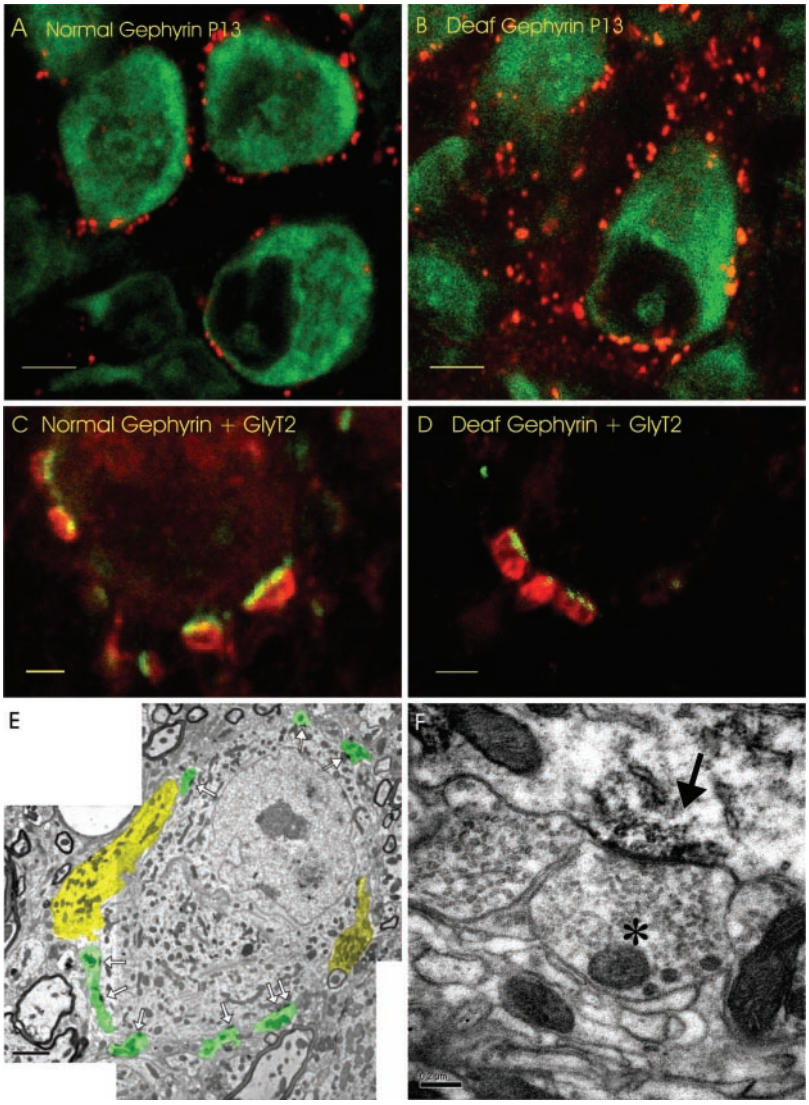

FIG. 2. Immunolabeling shows more inhibitory synapses on MNTB neurons from deaf mice compared with normal mice. MNTB neurons were immunolabeled with antibodies to the glycine receptor clustering protein gephyrin (mAb 7a). Confocal images (single optical sections) showing punctate gephyrin clusters (red dots; Cy3-fluorescence) on MNTB neurons (green fluorescence; Nissl stain) in normal mice (*A*) and deaf mice (*B*), at 13 days postnatal age. On average, MNTB neurons in deaf mice displayed a significantly larger number of discrete gephyrin clusters than neurons in normal mice (means ± SD; 61.9 ± 10.5, $n = 20$ cells versus 47.9 ± 7.1, $n = 20$ cells; $P < 0.01$; total number of clusters $n = 2295$). Dual immunolabeling for gephyrin (green) and GlyT2 (red) reveals that each gephyrin cluster is apposed by a glycinergic presynaptic bouton. Images are single optical sections from normal (*C*) and deaf (*D*) mice, respectively. *E*: ultrastructural localization of gephyrin clusters (arrows) on an MNTB neuron soma from a deaf mouse (13 days old) indicates that each surface membrane cluster is associated with a noncalyceal presynaptic nerve terminal (shaded green). Portions of the calyx of Held are shaded yellow. *F*: high magnification confirms that gephyrin immunoreactivity is specifically localized at the postsynaptic membrane, in association with relatively small axosomatic boutons (asterisk). The postsynaptic membrane associated with an adjacent small terminal is unlabeled.

immunolabeling observation (Fig. 2) that there are significantly more inhibitory synaptic specializations on the surface of MNTB neurons in deaf versus normal mice.

Figure 3*B* shows that mean mIPSC amplitude is significantly smaller in deaf mice compared with normal mice (deaf, 64.05 ± 2.26 pA, $n = 18$ cells; normal, 106.14 ± 3.5 pA, $n = 18$ cells; $P < 0.01$). Figure 3, *C* and *D*, illustrates histograms and cumulative distributions of mIPSC amplitudes for normal and deaf mice. These distributions were statistically different (Kolmgorov–Smirnov test, $P < 0.01$).

Glycinergic mIPSCs exhibit a slower time course in deaf mice

In addition to mIPSC amplitude and frequency, the time course of mIPSCs differed between normal and deaf mice (Fig. 4). Although the mean rise time of mIPSCs was not different between normal and deaf mice (normal, 0.42 ± 0.05 ms, $n = 18$ cells; deaf, 0.49 ± 0.02 ms, $n = 18$ cells; $P > 0.05$), mean mIPSC half-width was significantly longer for deaf versus normal mice (Fig. 4; normal, 2.28 ± 0.08 ms, $n = 18$ cells; deaf, 2.91 ± 0.11 ms, $n = 18$; $P < 0.01$).

Mean single glycinergic channel conductance is greater in deaf mice

Peak-scaled nonstationary fluctuation analysis of mIPSCs (Traynelis et al. 1993) was used to estimate the mean single channel current underlying the mIPSCs. This technique provides a weighted mean of the underlying multiple conductance states of the channels and may be used if there is no correlation between mIPSC amplitude and time course. Figure 5, *A* and *C*, illustrates examples of scatter plots for decay time constant versus amplitude for mIPSCs recorded in MNTB neurons from a normal (CBA) and a deaf (*dn/dn*) mouse, showing a lack of correlation (Spearman test, $P > 0.05$). (A lack of correlation was also evident for rise time versus half-width plots.) Figure 5, *B* and *D*, shows variance–mean mIPSC plots for a normal (CBA) and a deaf (*dn/dn*) mouse. The mean single channel currents for these two cells were calculated as 3.0 pA (normal) and 4.5 pA (deaf). Overall, the mean single channel current for deaf mice was significantly greater than for normal mice (deaf, 4.52 ± 0.06 pA, $n = 9$ cells; normal, 3.15 ± 0.05, $n = 9$ cells; $P < 0.03$; holding potential = −60 mV), corresponding to mean single

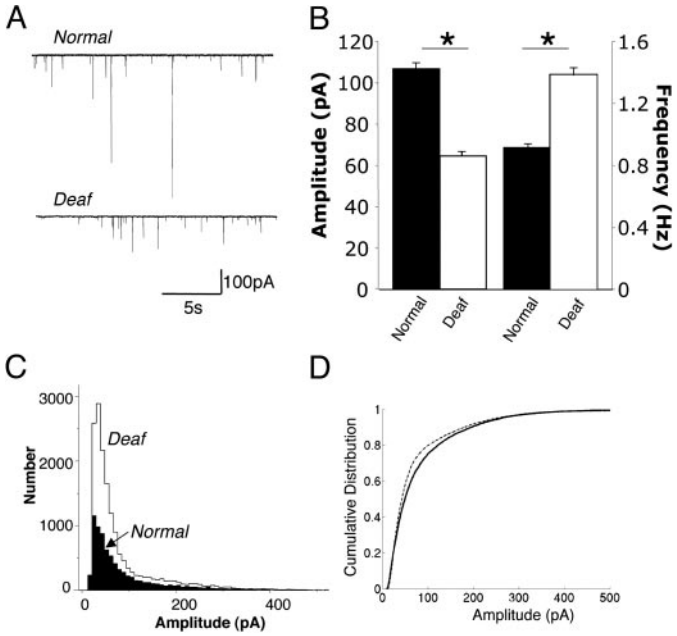

FIG. 3. Glycinergic mIPSCs in MNTB neurons from deaf mice are more frequent and exhibit a smaller mean amplitude than for normal mice. *A*: example traces of whole cell recordings of glycinergic mIPSCs in MNTB neurons from normal mice (*top*) and deaf (*bottom*) mice. *B*: mean amplitude and frequency of mIPSCs recorded in 18 MNTB cells from normal mice and 18 MNTB cells from deaf mice. *C*: histograms of mIPSC amplitudes in deaf mice ($n = 18$ cells, total number of mIPSCs = 14,275) and normal mice ($n = 18$ cells, total number of mIPSCs = 8792). *D*: cumulative amplitude distributions of the mIPSC shown in *C*, for deaf mice (broken line) and normal mice (continuous line).

channel conductances of 64.0 ± 0.84 pS (deaf) and 44.7 ± 0.75 pS (normal).

DISCUSSION

Previous studies have shown that disruption of auditory activity of cochlear origin may have a variety of central effects, including changes in cell metabolism and survival, protein synthesis, synaptic morphology and connectivity, and neuronal membrane properties (Francis and Manis 2000; Friauf and Lohmann 1999; Rubel and Fritzsch 2002). However, there is relatively little information on the effects of cochlear dysfunction at the detailed synaptic level in central auditory brain stem nuclei. Excitatory synaptic transmission between auditory nerve fibers and AVCN bushy cells in congenitally deaf mice is greater than in normal mice, due largely to a greater presynaptic release probability, without a change in quantal size (Oleskevich and Walmsley 2002). In the present study, we have investigated inhibitory synaptic transmission at the quantal level by recording spontaneous glycinergic mIPSCs in the MNTB. In contrast to miniature (m) EPSCs (Oleskevich and Walmsley 2002), our results demonstrate that there are significant differences, on average, in amplitude, time course, and frequency of glycinergic mIPSCs between normal and congenitally deaf *dn/dn* mice, at the same postnatal age (12–14 days).

The frequency of glycinergic mIPSCs is approximately 50% greater in deaf versus normal mice. The scaffolding protein gephyrin is involved in the clustering of postsynaptic glycine (and GABA) receptors, and our immunolabeling results demonstrated that the cell bodies of MNTB neurons contain many gephyrin clusters. At the ultrastructural level, it was confirmed that each of these clusters is localized in the postsynaptic surface membrane and represents the location of a separate synaptic specialization. In particular, the gephyrin immunolabeling is specifically associated with small presumed inhibitory synapses and not with the calyx of Held or with extrasynaptic membrane nor is it found in presynaptic structures around MNTB neurons. Interestingly, there are 30% more receptor clusters on the cell bodies of MNTB neurons in deaf mice compared with normal mice. The association of the gephyrin clusters with inhibitory synapses was further confirmed by dual immunostaining to visualize glycinergic and GABAergic presynaptic terminals in apposition to the surface membrane gephyrin. Although it is not yet known precisely to what extent glycine and GABA colocalize in these presynaptic terminals, or the degree of colocalization of the respective postsynaptic receptors, the relative proportion of gephyrin clusters apposed by glycinergic (GlyT2) or GABAergic (GAD65 or GAD67) synapses was unchanged in deaf versus normal MNTB neurons. Therefore a likely contribution to the increased frequency of mIPSCs in deaf mice is a greater total number of glycinergic synapses contacting MNTB neurons in the deaf mice.

The mean peak amplitude of glycinergic mIPSCs was found to be significantly smaller (60% of control) in deaf mice compared with normal mice. This may be due to presynaptic differences in the transmitter content of vesicles or to postsynaptic differences in the number of available postsynaptic receptors or the intrinsic properties of the receptor-channels (or a combination of these factors). Fluctuation analysis of mIPSCs showed that the weighted mean single channel conductance was greater for deaf mice (64 pS) than for normal mice (45 pS), indicating that the decreased mean amplitude mIPSC in deaf mice is not due to a smaller single channel conductance. These values for mean single channel conductance are similar to previously reported values for heteromeric glycine receptors (42–54 pS) (Rajendra et al. 1997). Singer and Berger (1999) did not find a developmental change in mean single channel conductance of glycine receptors in brain stem motoneurons, despite a developmental change in subunit composition. However, larger mean single channel conductances have been reported for homomeric versus heteromeric glycine receptors (Rajendra et al. 1997), and it is possible that there is a contribution of homomeric channels to the mIPSCs in deaf mice.

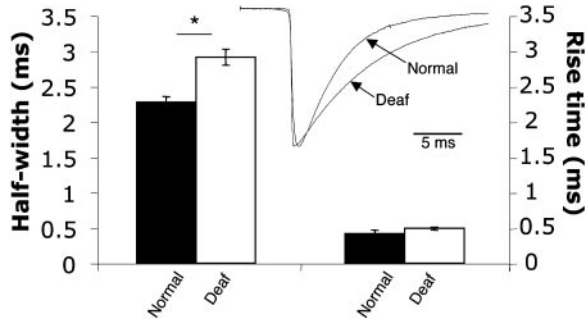

FIG. 4. Decay time course is slower for mIPSCs recorded in MNTB neurons from deaf mice compared with normal mice. Inset shows examples of mean mIPSCs normalized to the same peak amplitude from a deaf mouse and a normal mouse. Bar graph (*right*) shows no significant difference in mean mIPSC rise times between normal ($n = 18$ cells) and deaf mice ($n = 18$ cells). Bar graph (*left*) shows that the mean half-width is significantly greater for mIPSCs in deaf mice ($n = 18$ cells) vs. normal mice ($n = 18$ cells).

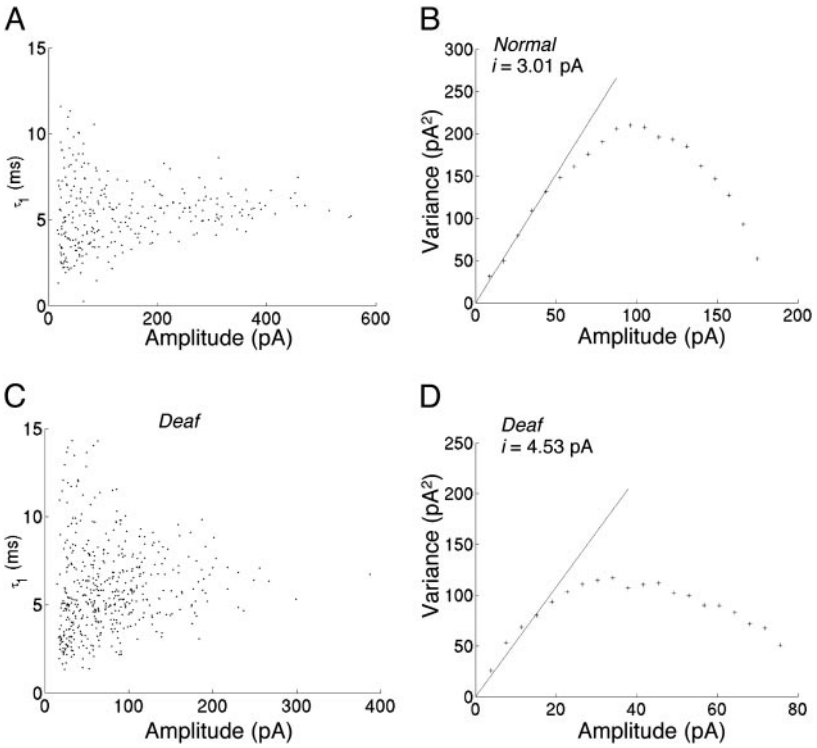

FIG. 5. Fluctuation analysis shows that the mean single channel current underlying mIPSCs is greater for deaf mice vs. normal mice. Examples showing no significant correlation in amplitude–decay time constant plots for mIPSCs recorded in MNTB neurons from a normal mouse (*A*) and a deaf mouse (*C*). Variance–amplitude plots for the same cells as in *A* and *B* (see text for explanation). Single channel current was calculated from the initial slope of the variance–amplitude plots (*B* and *D*, straight lines). On average, mean single channel current was significantly greater for deaf mice than for normal mice (deaf, 4.52 ± 0.06 pA, $n = 9$ cells; normal, 3.15 ± 0.05, $n = 9$ cells; $P < 0.05$).

Based on the mean single channel conductances, the number of channels open at the peak of the mean mIPSC was calculated to be 34 channels for normal mice and 14 for deaf mice. A similar range of channel numbers was found by Singer and Berger (1999), who reported that glycinergic mIPSCs in rat hypoglossal motoneurons are generated by a mean of 12 channels for neonates (P0–3) and 24 channels for juvenile rats (P11–18). They proposed that this difference is primarily due to a greater number of available glycine receptors in juvenile rats compared with neonatal rats (Singer and Berger 1999). A smaller number of available receptors could also underlie the smaller mean mIPSC amplitude in MNTB neurons of deaf compared with normal mice in the present study.

Previous studies have shown that, during the first two weeks postnatal, there is a developmental change in the subunit composition of glycine receptors, in which the fetal α2-subunit is replaced by the adult α1-subunit (Friauf et al. 1997; Kungel and Friauf 1997). This subunit switch results in a change in receptor-channel kinetics, which has been observed as a developmental reduction in the decay time constant of mIPSCs in a variety of cell types (Krupp et al. 1994; Singer et al. 1998; Takahashi et al. 1992). Kungel and Friauf (1997) reported developmental changes in the physiology and pharmacology of glycine receptors during the first 2 wk postnatal in rat MNTB neurons. Before P4, MNTB neurons express a mixture of α2-homomers and α2/β-heteromers but, in the second week postnatal, the α1-subunit–containing glycine receptors predominate (Kungel and Friauf 1997). Our results demonstrate that the mIPSC decay time course is slower in MNTB neurons of deaf mice compared with normal mice, at 12–14 days postnatal. A likely explanation for the difference in mIPSC time course between normal and deaf mice is a higher proportion of α2/β-heteromeric receptors at synapses in deaf mice compared with normal mice. A potential pharmacological means of examining further the glycine receptor subunit composition is the use of the compound cyanotriphenylborate (CTB) (Kungel and Friauf 1997; Smith et al. 2000). CTB was used in these studies to distinguish between α1- and α2-subunit–containing glycine receptors, as it preferentially blocks α1-subunit–containing receptors.

Previous studies have demonstrated that both activity-dependent and activity-independent processes regulate the formation of auditory circuits and synaptic and neuronal properties (Francis and Manis 2000; Friauf and Lohmann 1999; Rubel and Fritzsch 2002). Many previous studies have used unilateral or bilateral cochlear ablation to study the effects of changes in auditory nerve activity, and some of these studies have specifically investigated glycinergic transmission (e.g., Kotak and Sanes 1996; Vale and Sanes 2000, 2002). A variety of effects of cochlear ablation on glycinergic transmission have been observed, including changes in the density of glycine receptors (Koch and Sanes 1998; Suneja et al. 1998) and a reduction in the amplitude of evoked glycinergic IPSCs (Kotak and Sanes 1996). Sanes and Takacs (1993) examined the terminal arborizations of (glycinergic) MNTB neurons and found that terminal sprouting occurred in response to functional denervation of these neurons. Suneja et al. (1998) examined strychnine binding following unilateral cochlear ablation and found evidence for a decreased expression of glycine receptors in the ipsi- and contralateral cochlear nuclei, but an elevation in the contralateral superior olivary complex. In our investigations, we have used congenitally deaf mice in which both spontaneous and evoked auditory nerve activity is disrupted, due to dysfunctional hair cell–spiral ganglion cell transmission. This provides a naturally occurring model that may provide valuable insights into central aspects of human congenital deafness, in addition to the central consequences of a lack of auditory nerve activity. Our results have demonstrated a smaller quantal am-

plitude and slower time course of glycinergic mIPSCs and a larger underlying single channel conductance in the MNTB of congenitally deaf mice. In addition, our immunolabeling revealed a significantly larger number of inhibitory synaptic sites contacting MNTB neurons in deaf mice, correlating with a greater frequency of mIPSCs in these cells. These results indicate that complex central changes at the fundamental synaptic level are associated with peripheral cochlear dysfunction, with some of these effects apparently opposing each other (e.g., smaller quantal size but a greater number of synaptic contacts). In addition, the results are likely to be relevant to our understanding of the central changes underlying human hereditary deafness.

ACKNOWEDGMENTS

The authors are grateful to Drs. J. Bekkers and A. Berntson for helpful comments on an earlier draft of the manuscript, to K. Steel and N. Glenn (MRC Institute of Hearing Research, Nottingham, UK) for providing the *dn/dn* mice, and to K. Matthaei (Gene Targeting Group, JCSMR, ANU) for help and advice.

GRANTS

This work was partly supported by National Institute of Neurological Disorders and Stroke Grant NS-25547 to R. Fyffe.

REFERENCES

Alvarez FJ, Dewey DE, Harrington DA, and Fyffe REW. Cell-type specific organization of glycine receptor clusters in the mammalian spinal cord. *J Comp Neurol* 379: 150–170, 1997.

Bock GR, Frank MP, and Steel KP. Preservation of central auditory function in the deafness mouse. *Brain Res* 239: 608–612, 1982.

Chattipakorn SC and McMahon LL. Pharmacological characterization of glycine-gated chloride currents recorded in rat hippocampal slices. *J Neurophysiol* 87: 1515–1525, 2002.

Clements JD and Bekkers JM. Detection of spontaneous synaptic events with an optimally scaled template. *Biophys J* 73: 220–229, 1997.

Craig AM. Activity and synaptic receptor targeting: the long view. *Neuron* 21: 459–462, 1998.

Durham D, Rubel EW, and Steel KP. Cochlear ablation in deafness mutant mice: 2-deoxyglucose analysis suggests no spontaneous activity of cochlear origin. *Hear Res* 43: 39–46, 1989.

Forsythe ID and Barnes-Davies M. The binaural auditory pathway: excitatory amino acid receptors mediate dual timecourse excitatory postsynaptic currents in the rat medial nucleus of the trapezoid body. *Proc R Soc Lond B Biol Sci* 251: 151–157, 1993.

Francis HW and Manis PB. Effects of deafferentation on the electrophysiology of ventral cochlear nucleus neurons. *Hear Res* 149: 91–105, 2000.

Friauf E, Hammerschmidt B, and Kirsch J. Development of adult-type inhibitory glycine receptors in the central auditory system of rats. *J Comp Neurol* 385: 117–134, 1997.

Friauf E and Lohmann C. Development of auditory brainstem circuitry: activity-dependent and activity independent processes. *Cell Tissue Res* 297: 187–195, 1999.

Helfert RH, Bonneau JM, Wenthold RJ, and Altschuler RA. GABA and glycine immunoreactivity in the guinea pig superior olivary complex. *Brain Res* 501: 269–286, 1989.

Isaacson JS and Walmsley B. Counting quanta: direct measurements of transmitter release at a central synapse. *Neuron* 15: 875–884, 1995.

Kandler K and Friauf E. Development of glycinergic and glutamatergic synaptic transmission in the auditory brainstem of perinatal rats. *J Neurosci* 15: 6890–6904, 1995.

Keats BJ and Berlin CI. Genomics and hearing impairment. *Genome Res* 9: 7–16, 1999.

Kim G and Kandler K. Elimination and strengthening of glycinergic/GABAergic connections during tonotopic map formation. *Nature Neurosci* 6: 282–290, 2003.

Kirsch J and Betz H. Glycine-receptor activation is required for receptor clustering in spinal neurons. *Nature* 392: 717–720, 1998.

Koch U and Sanes DH. Afferent regulation of glycine receptor distribution in the gerbil LSO. *Microsc Res Tech* 41: 263–269, 1998.

Kotak VC, Korada S, Schwartz IR, and Sanes DH. A developmental shift from GABAergic to glycinergic transmission in the central auditory system. *J Neurosci* 18: 4646–4655, 1998.

Kotak VC and Sanes DH. Developmental influence of glycinergic transmission: regulation of NMDA receptor-mediated EPSPs. *J Neurosci* 16: 1836–1843, 1996.

Krupp J, Larmet Y, and Feltz P. Postnatal change of glycinergic IPSC decay in sympathetic preganglionic neurons. *Neuroreport* 5: 2437–2440, 1994.

Kungel M and Friauf E. Physiology and pharmacology of native glycine receptors in developing rat auditory brainstem neurons. *Dev Brain Res* 102: 157–165, 1997.

Lim R, Alvarez FJ, and Walmsley B. Quantal size is correlated with receptor cluster area at glycinergic synapses in the rat brainstem. *J Physiol* 516: 505–512, 1999.

Lim R, Alvarez FJ, and Walmsley B. GABA mediates presynaptic inhibition at glycinergic synapses in a rat auditory brainstem nucleus. *J Physiol* 525: 447–459, 2000.

Lim R, Oleskevich S, Few A, Leao R, and Walmsley B. Glycinergic mIPSCs in mouse and rat brainstem auditory nuclei: modulation by ruthenium red and the role of calcium stores. *J Physiol* 546: 691–699, 2003.

Oleskevich S and Walmsley B. Synaptic transmission in the auditory brainstem of normal and congenitally deaf mice. *J Physiol 540*: 447–455, 2002.

Rajendra S, Lynch JW, and Schofield PR. The glycine receptor. *Pharmacol Ther* 73: 121–146, 1997.

Rubel EW and Fritzsch B. Auditory system development: primary auditory neurons and their targets. *Annu Rev Neurosci* 25: 51–101, 2002.

Sanes DH and Friauf E. Development and influence of inhibition in the lateral superior olivary nucleus. *Hear Res* 147:46–58, 2000.

Sanes DH and Takacs C. Activity-dependent refinement of inhibitory connections. *Eur J Neurosci* 5: 570–574, 1993.

Schneggenburger R, Sakaba T, and Neher E. Vesicle pools and short-term synaptic depression: lessons from a large synapse. *Trends Neurosci* 25: 206–212, 2002.

Singer JH and Berger AJ. Contribution of single-channel properties to the time course and amplitude variance of quantal glycine currents recorded in rat motoneurons. *J Neurophysiol* 81: 1608–1616, 1999.

Singer JH, Talley EM, Bayliss DA, and Berger AJ. Development of glycinergic synaptic transmission to rat brain stem motoneurons. *J Neurophysiol* 80: 2608–2620, 1998.

Smith AJ, Owens S, and Forsythe ID. Characterisation of inhibitory and excitatory postsynaptic currents of the rat medial superior olive. *J Physiol* 529: 681–698, 2000.

Steel KP and Bock GR. The nature of inherited deafness in deafness mice. *Nature* 288: 159–161, 1980.

Suneja SK, Benson CG, and Potashner SJ. Glycine receptors in adult guinea pig brain stem auditory nuclei: regulation after cochlear ablation. *Exp Neurol* 154: 473–488, 1998.

Takahashi T, Momiyama A, Hirai K, Hishinuma F, and Akagi H. Functional correlation of fetal and adult forms of glycine receptors with developmental changes in inhibitory synaptic receptor channels. *Neuron* 9: 1155–1161, 1992.

Traynelis SF, Silver RA, and Cull-Candy SG. Estimated conductance of glutamate receptor channels activated during EPSCs at the cerebellar mossy fiber-granule cell synapse. *Neuron* 11: 279–289, 1993.

Vale C and Sanes DH. Afferent regulation of inhibitory synaptic transmission in the developing auditory midbrain. *J Neurosci* 20: 1912–1921, 2000.

Vale C and Sanes DH. The effect of bilateral deafness on excitatory and inhibitory synaptic strength in the inferior colliculus. *Eur J Neurosci* 16: 2394–2404, 2002.